Analytical Methods

Accepted Manuscript

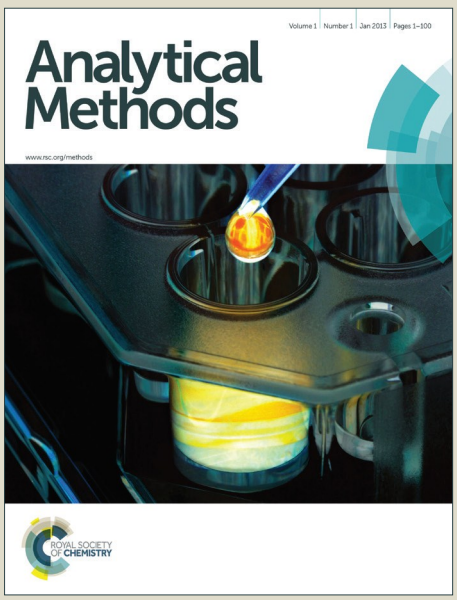

This is an *Accepted Manuscript*, which has been through the Royal Society of Chemistry peer review process and has been accepted for publication.

Accepted Manuscripts are published online shortly after acceptance, before technical editing, formatting and proof reading. Using this free service, authors can make their results available to the community, in citable form, before we publish the edited article. We will replace this *Accepted Manuscript* with the edited and formatted *Advance Article* as soon as it is available.

You can find more information about *Accepted Manuscripts* in the Information for Authors.

ROYAL SOCIETY OF CHEMISTRY

www.rsc.org/methods

Developing a nanostructure electrochemical sensor for simultaneous determination of cysteine and tryptophan

Ali Benvidi[1*], Mohammad M. Ansaripour, Nooshin Rajabzadeh, Hamid R. Zare, Bi-Bi Fatemeh Mirjalili

Department of Chemistry, Faculty of Science, Yazd University, Yazd 89195-741, Iran

Abstract

A modified carbon paste electrode (CPE) was prepared based on a newly synthesized compound of 14-(4-Hydroxyphenyl)-14-H-dibenzo [a,j]-xanthene (HDX) and multi-wall carbon nanotubes (MWCNTs). At first, the redox properties of the modified electrode were studied by cyclic voltammetry (CV). Then, the modified electrode was used as an electrochemical sensor for oxidation of cysteine (Cys). Under the optimum pH of 8.5, the overpotential of Cys oxidation decreased about 280 mV at the modified electrode rather than at an unmodified CPE. The differential pulse voltammetry (DPV) of Cys at the electrochemical sensor exhibited two linear dynamic ranges with a detection limit ($3s_b$) of 1.0 μM. Also, DPV was used for simultaneous determination of Cys and tryptophan (Try) by the electrochemical sensor. The proposed electrochemical sensor was used for determination of these substances in real samples (i.e. tablets and human serums).

Keywords: Voltammetry, Carbon paste electrode, Multi-wall carbon nanotube, Cysteine, Tryptophan

*[1]Corresponding author: Tel.: +98 351 8122645; Fax: 98 351 8210644.

e-mail address: abenvidi@yazd.ac.ir, benvidi89@gmail.com

1. Introduction

As compared to other instrumental analytical methods, using electrochemical sensors constructed with modified electrodes has proved to be an inexpensive and simple analytical method that has remarkable detection sensitivity and allows for reproducibility and easy miniaturization.[1-6] Nanomaterials in electrochemically modified electrodes are considerable in that they facilitate the transfer of electrons and provide large catalytic surface areas.[7,8] They have unique physical and chemical properties such as high sensitivity, stability, and high conductivity. Multi-Wall Carbon Nanotubes (MWCNTs) are the interesting members of the carbon family offering unique mechanical and electronic properties combined with their chemical stability. A good deal of experimental and theoretical research has been directed towards their production and purification. Also, their mechanical and electronic properties as well as their electrical conductivity have been extensively investigated.[5-8]

L-Cysteine (l-2-amino-3-mercaptopropionic acid) is a sulfur-containing amino acid. The sulphydryl (-SH) group of cysteine plays a key role in the biological activity of protein and enzymes.[9,10] It has been used as a radio-protective agent and a cancer indicator. It is also implicated in a number of pathological conditions, including Alzheimer's and Parkinson's diseases as well as autoimmune deficiency syndrome.[11-13] L-cysteine is widely used in the food industry as an antioxidant, in the pharmaceutical industry in drug formulation and as a biomarker.[14] On the other hand, deficiency of L-cysteine causes many diseases such as low growth in children, depigmentation of hair, edema, lethargy, liver damage, loss of muscle and fat, skin lesion and weakness.[15] Therefore, measuring L-cysteine in body fluids is very important

from biological and pharmacological stand points, where many efforts have been made to develop sensitive methods for its detection. For its determination, several methods have been reported, including chemiluminescence[13], high-performance liquid chromatography[16], fluorimetry[17] and electrochemistry.[18,19]

Try is an angiotensin-converting enzyme inhibitor used for the treatment of hypertension and some types of congestive heart failure. It is an essential amino acid with diverse physiological roles, functioning both independently or via incorporation into the structure of larger molecules or polymers, such as proteins. It has been shown that the control of dietary intake of Try through food or supplements has a positive effect on the regulation of serotonin synthesis.[20] Try is a precursor for biologically important molecules, such as the neurotransmitter serotonin and the neurohormone melatonin.[21] Abnormal levels of serotonin and melatonin have been shown to be associated with depression, Alzheimer's and Parkinson's diseases respectively. The regulation of the synthesis of serotonin leads to the controlled synthesis of melatonin[22] which promotes sleep. Following the lifting of the USA Food and Drug Association ban on Try, this amino acid has been increasingly available in food supplement forms, and in some formulations co-administered with melatonin. Given the far-reaching role of this amino acid, methods for its detection in food processing, pharmaceutical formulations and biological fluids are of great importance.[23] Electrochemical methods of detecting Try have been shown to be promising as compared to standard chromatographic and electrophoretic methods.[24-27] As mentioned above, Cys and Try are amino acids that play a critical roles in processes such as neurotransmitter transport and biosynthesis. Also, the voltammetric determination of Cys and Try is often interfered by some coexisting substances in biological systems, such as ascorbic acid (AA) and uric acid (UA). This is why development of a selective method for the simultaneous determination of Cys and Try has

appeared to be of great importance because of their coexistence in biological systems and pharmaceutical preparations. Therefore, it is important to establish a sensitive, selective, fast and simple method for detection of Cys and Try contents in real samples such as tablets and human serums.

In this paper, at first, the electrochemical behavior of 14-(4-Hydroxyphenyl)-14-H-dibenzo [a,j]-xanthene (HDX) is investigated. To the best of our knowledge, there is no report in the literature about the simultaneous determination of these compounds by voltammetry based on HDX-MWCNPs modified carbon paste electrodes (HDX/MWCNT/CPE). We prepare a novel nanostructure electrochemical sensor for the simultaneous determination of Cys and Try. The experimental results indicate that the modified electrode offers several advantages such as high repeatability, good stability and high apparent charge transfer rate constant. Also, the electro catalytic effect of the modified electrode (HDX/MWCNT/CPE) is described for the individual and simultaneous determinations of Cys and Try. Using the developed method, the determination of the two compounds is carried out in tablets and human blood serum samples.

2. Experiment

2.1. Instruments and chemicals

Voltammetric measurements were carried out using a computerized potentiostat/galvanostat (SAMA 500 Electro analyzer system, Iran). All the electrochemical studies were performed at 25ºC ± 1ºC. A three-electrode assembly was employed for the experiment in a 50 mL glass cell containing an Ag/AgCl electrode as a reference electrode, a platinum wire counter electrode and

a modified multi-wall carbon nanotube paste electrode as a working electrode. All of the potentials were measured and reported versus the Ag/AgCl reference electrode. A Metrohm 691 pH/ion meter was also used for pH measurements. All of the solutions were freshly prepared using doubly distilled water. Cysteine, tryptophan and reagents were of analytical grades from Merck. Fine graphite powder (Merck) and paraffin oil (DC 350, Merck, density = 0.88 g cm^{-3}) were used as binding agents for the graphite pastes. The multi-wall carbon nanotubes (Outer diameter: 5-20 nm; inner diameter: 2-6 nm; length: 1-10 µm and 95% pure) were purchased from Plasma Chem (Germany). Before use, flasks and containers were soaked in 6 M HNO_3 for at least 24 hours, then rinsed with deionised water. The buffer solutions were prepared from ortho-phosphoric acid and its salts in the pH range from 5.00 to 12.00.

2.2. Synthesis of 14-(4-Hydroxyphenyl)-14*H*-dibenzo [a,j]-xanthene (HDX)

A mixture of 2-naphthol (2 mmol), 4-hydroxy benzaldehyde (1 mmol) and nano-$SnCl_4$. SiO_2(0.015 g) was heated at 80 ˚C. The progress of the reaction was monitored by TLC. After completion of the reaction, the mixture was washed with chloroform and filtered to recover the catalyst. The filtrate was evaporated, and the crude product was recrystallized from *iso*-propanol and chloroform (80:20) to afford the product in 85 yields.[28]

2.3. Preparation of the modified electrode

To obtain the best conditions in the preparation of HDX/MWCNT/CPE, we optimized the ratio of HDX, MWCNT and graphite powder. The results of our study showed that the maximum

peak current intensity of Cys could be obtained at the surface of HDX/MWCNT/CPE with the optimum ratio of HDX and MWCNTs. HDX/MWCNT/CPE was prepared by dissolving 0.012 g of HDX in methylene chloride and hand mixing it with 0.246 g of graphite powder and 0.004 g of MWCNTs using a mortar and pestle. Then, ~0.7 mL of paraffin was added to the above mixture and mixed for 20 min until a uniformly wetted paste was obtained. The paste was then packed into the end of a glass tube (ca. 3.4 mm i.d. and 10 cm long). A copper wire inserted into the carbon paste provided the electrical contact. When necessary, a new surface was obtained by pushing an excess of the paste out of the tube and polishing it with a weighing paper. For comparison, HDX-modified CPE (HDX/CPE) without MWCNTs, MWCNT paste electrode (MWCNT/CPE) without HDX, and unmodified CPE in the absence of both HDX and MWCNT were also prepared in the same way.

Fig. 1 displays a typical morphology of CPE (A), CPE/MWCNT (B) and CPE/MWCNT/HDX (C). Fig. 1A shows the SEM of graphite. This figure shows that graphite is characterized by a surface formed by irregularly shaped flakes of graphite that were isolated and each layer could be clearly distinguished[29]. As seen in this figure, there is not any particle in nano scale. After addition of MWCNTs to carbon paste matrix, it can be seen that MWCNTs were distributed on the surface of electrode with a special three-dimensional structure, indicating that MWCNTs were successfully assimilated on the electrode[29] (Fig. 1B). By adding MWCNTs, carbon fibers in nano scale can be observed in the figure. Comparing this figure with previous one indicated that carbon nano tubes have been added to graphite. Fig. 1C exhibits the SEM image of Graphite/MWCNT/HDX. The Fig. 1B and Fig. 1C are the same, because of the fact that, the molecular size of HDX is smaller than 50 nm, SEM has not enough resolution for distinguishing of this size. So, there is no difference in these two pictures.

Fig. 2 shows the infrared spectra of Graphite, Graphite/MWCNT and Graphite/MWCNT/HDX. As it is expected, no significant peak is found in FT-IR spectrum of graphite. As the inset of Fig. 2 shows, in the FT-IR spectrum of MWCNTs, a weak absorption peak observed in about 1560 cm^{-1} is more likely from C=C stretching mode of MWCNTs.[30] By adding HDX, due to the presence of modifier functional groups, the infrared spectra peaks are appeared that are in accordance to the HDX structure. In comparison with the modifier peaks, the MWCNT peaks are not observed due to presence of high intensity peaks of modifier functional groups.

By adding HDX, due to the presence of modifier functional group, the infrared spectra peaks are appeared that are in accordance to the HDX structure.

Also, the quantitative surface analysis was performed by energy-dispersive X-ray spectroscopy (EDX) approach. EDX is an analytical technique used for the elemental analysis or chemical characterization of a sample. The EDX spectra of Graphite, Graphite/MWCNT and Graphite/MWCNT/HDX have been shown at the Fig. 3. In the figure, X axis shows energy (eV) and Y axis exhibits peak intensity. As expected, in the structures of graphite and carbon nano tubes another element does not exist except carbon, so the EDX spectra in Fig. 3A and 3B are indicating presence of carbon. The EDX spectrum of Graphite/MWCNT/HDX has been shown at the Fig. 3C. The results of quantitative elemental analysis are indicating the presence of C and O in Graphite/MWCNT/HDX. Whereas the modifier structure only contains three elements (carbon, hydrogen and oxygen) and hydrogen does not show any peak in EDX spectra and EDX peaks of carbon and oxygen are appeared under than 2.0 KeV, so we showed the EDX spectra in the range of 0.0 to 3.0 KeV. Elemental analysis using EDX spectra peaks confirms the presence of carbon and oxygen which is in agreement with HDX structure.

2.4. Real samples

Four tablets of Cys were weighed and ground well. A sufficient amount of this powder was dissolved in 0.1 M of a phosphate buffer solution to obtain a stoke solution with the concentration of about 0.01 M. After adjusting the pH (pH=8.5), further dilution was performed to reach the calibration range of Cys.

A simulated serum sample was prepared according to a real serum sample. After adjusting the pH using a phosphate buffer solution (pH=8.5), different amounts of Cys were spiked to the sample. Then, 10 mL of the solution was transferred into a voltammetric cell to be analyzed without any further pretreatment.

3. Results and discussion

3.1. Electrochemical behaviour

To the best of our knowledge, there is no prior report in the literature on the electrochemical properties and, in particular, the electrocatalytic activity of HDX in aqueous media. Since HDX complex is insoluble in aqueous solutions, it can be used in a carbon paste without leaching out from the electrode surface, which leads to a stable chemically modified electrode. Therefore, we prepared modified electrodes based on HDX/MWCNT/CPE and studied their electrochemical properties in a buffered aqueous solution (pH = 8.5). The effect of the potential scan rate (υ) on the electrochemical properties of HDX/MWCNT/CPE was also studied by CV. Plots of the anodic peak currents (I_{pa}) were linearly dependent on υ in the range of 10–600 mV s^{-1} (Fig. 4A), indicating that the redox process is controlled in a diffusion-independent manner for a surface-

confined redox process. An approximate estimate of the surface coverage of the electrode was made by adopting the method used by Sharp.[31] According to this method, the peak current is related to the surface concentration of the electroactive species, Γ, calculated through the following equation:

$$I_p = n^2F^2A\Gamma v/4RT \quad (1)$$

where n represents the number of electrons involved in the reaction, A is the surface area (0.096 cm^2) of the electrode, Γ (mol cm^{-2}) is the surface coverage, and the other symbols have their usual meanings. Based on the slope of the anodic peak currents versus the scan rate (Fig. 4A), the calculated surface concentration is 1.6×10^{-10} mol cm^{-2} for n = 2.

The transfer coefficient, α, of the surface-confined redox couple was evaluated from CV experiments using the variation of the anodic peak potentials with the logarithm of the scan rate. This was done by employing the procedure of Laviron.[32] We realized that, for scan rates higher than 300 mV s^{-1} , the E_{pa} values are proportional to the logarithm of the potential scan rate (Fig. 4B). The slopes of the plots can be used to extract the kinetic parameter α. The slope of the linear segment is equal to $2.303RT/(1-\alpha_a)\ n_\alpha F$ for the anodic peaks. The calculated value for the average transfer coefficient (α) is 0.41.

The electrochemical behavior of HDX/MWCNT/CPE was studied at different pHs using the CV method. As shown in Fig. 4C, the formal potential ($E^{o\prime}$) of HDX/MWCNT/CPE is pH-dependent. Since just one straight line is obtained with a slope value of -71.3 mV per pH in the pH range of 5.0–12.0, there is the same number of electrons and protons in the redox reaction of HDX in the pH range of 5.0–12.0. As can be seen in Scheme 1, for oxidation of one molecule of HDX, two electrons are needed; therefore, a two-electron/ two-proton process is supposed to be involved. These results are in accordance with the suggested mechanism shown in Scheme 1.

Here Figure 4

3.2. Electrocatalytic oxidation of cysteine at HDX/MWCNT/CPE

Electrocatalytic oxidation of Cys at HDX/MWCNT/CPE can be seen in Fig. 5. For a comparison of different electrodes, the CVs of HDX/MWCNT/CPE, HDX/CPE, and a bare CPE were tested in a buffered aqueous solution (pH=8.5) in the presence and absence of Cys. According to Fig. 5, curve b, oxidation of Cys did not occur on an unmodified electrode even in a high positive potential. A comparison of curves b, d and e in this figure shows a decrease in the over potential of Cys oxidation from 850 mV at a bare CPE (curve b) to 590 mV at HDX/CPE (curve d) and 570 mV at HDX/MWCNT/CPE (curve e). The comparison of these curves shows that the peak potential of Cys oxidation at HDX/MWCNT/CPE shifts about 280 mV towards a negative value as compared with that at the bare CPE. In addition, an approximately four-fold increase was observed in the oxidation peak current of Cys when HDX/MWCNT/CPE was used versus a bare CPE. A comparison of curves d and b in Fig. 5 demonstrates that the electro-oxidation of Cys can be catalyzed by HDX/CPE rather than CPE. This is because the anodic peak current of the modifier was increased highly by modification of the electrode. This behavior is typical of and expected for electro catalysis at chemically modified electrodes. Also, the comparison of Cys oxidation at HDX/MWCNT/CPE (curve e) and HDX/CPE (curve d) shows an enhancement of the peak current at the modified electrode, suggesting that it was the presence of MWCNT in the modified electrode that could enhance the peak current. Through these results, one may realize that MWCNT on a surface electrode can cause a great improvement in electrochemical

responses. This is due to the excellent characteristics of MWCNT such as high surface area, high chemical stability and good electrochemical conductivity.

The effect of pH was also investigated on the electrocatalytic oxidation of Cys. The inset of Fig. 5 shows that the optimum pH for the electro catalysis of Cys is 8.5. As Scheme 1 suggests, the electrooxidation of HDX and Sys is performed in the presence of protons. Therefore, the electrooxidation of Cys in pHs higher than 8.5 causes a decrease in the oxidation peak current. A decrease of the oxidation peak current in low-pH solutions is probably because of protonation of OH groups on the modifier or the amine group in Cys. Therefore, in this study, 8.5 was selected as the optimum amount of pH.

Here Figure 5

The effect of the concentration of Cys on the electrocatalytic properties of HDX/MWCNT/CPE was investigated in a 0.1 M phosphate buffer solution at the scan rate of 100 mVs^{-1} (Fig. 6). The inset A of Fig. 6 shows a Tafel plot that was drawn from the CV of 1.0 mM of Cys at the scan rate of 100 mVs^{-1}. A Tafel slope of 0.1076 V was obtained in this case, and the charge transfer coefficient was calculated to be $\alpha = 0.45$. As shown in the inset of Fig. 6, the peak current varies linearly with the square root of the scan rate. Based on inset B of Fig. 6, the anodic oxidation current of Cys is proportional to the square root of the scan rate, showing that the reaction is controlled by diffusion.[33]

Here Figure 6

3.3. Chronoamperometric measurements

Chronoamperometric measurements of Cys were made on HBX/MWCNT/CPE at the working electrode potential of 700 mV for various concentrations of Cys (Fig. 7). For Cys, as an electroactive material with a diffusion coefficient of D, the current observed for the electrochemical reaction in the mass transport limited condition is described by the Cottrell equation.[33] Experimental plots of I vs.$t^{-1/2}$ were employed, with the best fits for different concentrations of Cys. The slopes of the resulting straight lines were then plotted versus the Cys concentration (Fig. 7B). From the resulting slope and the Cottrell equation, the mean value of D was found to be (2.8×10^{-6} cm^2/s). The obtained value for the diffusion coefficient of Cys is comparable with the values reported in the literature.[34,35]

Here Figure 7

3.4. Calibration plot and limit of detection

DPV method was used to determine the concentration of Cys (Fig. 8). The plot of the peak current versus the Cys concentration consisted of two linear segments with slopes of 39.36 and 7.62 μA mM^{-1} in the concentration ranges of 4.0–80.0 μM and 80.0-1000 μM respectively. The decrease in the sensitivity (slope) of the second linear segment is likely due to kinetic limitation. Ten replicate measurements of a blank were obtained by the analytical method, the standard deviation was then calculated, and the responses were converted into concentration units. The obtained statistic concentration was multiplied by 3, and the result was the detection limit. The

detection limit (3s) of Cys was found to be 1.0 μM. In Table 1, some of the analytical characteristics obtained in this research are compared with those previously reported in the literature.[34-38] According to Table 1, the sensor prepared in our study has a better detection limit due to composite HBX and MWCNT (Except ref. 37) and a wider linear range as compared to the sensors reported by other studies. In addition, the over voltage decreased more in the present study than in most other studies.

Here Figure 8

Here Table 1

3.5. Interference study

The influence of various foreign species was investigated on the determination of 0.1 mM Cys. The tolerance limit was taken as the maximum concentration of the foreign substances, which caused an approximately ±5% relative error in the determination of Cys. The tolerated concentration of the foreign substances was 1.0×10^{-3} M for L-serine, tryptophan, guanine, folic acid, dopamine, glutamic acid, L-Alanine and L-histidine. Therefore, foreign species in a ratio of 10 times do not bear any influence on determination of Cys.

3.6. Simultaneous determination of Cys and Try

The differential pulse voltammograms of 500.0 μM Cys obtained at a bare CPE (curve d) and HBX/MWCNT/CPE (curve b) are compared in the inset of Fig. 9. As these curves show, Cys does not have any oxidation peak on the bare CPE. The differential pulse voltammograms of 500.0 μM Cys + 100.0 μM Try at the bare CPE and HBX/MWCNT/CPE are compared in the inset of Fig. 9. As it can be seen, HBX/MWCNT/CPE is able to separate the anodic oxidation peaks of Cys and Try (curve a), while the bare CPE is not (curve c). In addition, the oxidation potential of Try at HBX/MWCNT/CPE is observed at a higher potential as compared to the one at the bare CPE. These results suggest how important it is to modify the surface of electrodes using HBX/MWCNT for simultaneous determination of Cys and Try.

Simultaneous determination of Cys and Try by HBX/MWCNT/CPE was performed by simultaneously changing the concentrations of Cys and Try. The voltammetric results showed well-defined anodic peaks at the potentials of 500 and 780 mV, corresponding to the oxidation of Cys and Try respectively. This signifies that the simultaneous determination of these compounds can occur without any interference (Fig. 9)

Here Figure 9

3.7. Analytical applications

3.7.1. Analysis of Cys in tablets of acetyl cysteine

HBX/MWCNT/CPE was successfully applied to the direct determination of Cys in tablets of acetyl cysteine. The Cys contents in these tablets were determined by the standard addition method in order to prevent any matrix effect. The value of Cys was found to be 145 μM ± 2 (n=5) in Cys tablets. The obtained results were in good agreement with the true value (147 μM).

The t_{exp} value, based on the t-test[39] value, was calculated to be 2.60. Since t_{exp} was less than t_{cri} (t_{cri} =2.78), there is no chance of incidence to assume for any systematic error in the obtained results.

3.7.2. Determination of Cys and Try in human blood serum samples

In order to evaluate the analytical applicability of the proposed method, it was used for the determination of Cys in human blood serum samples (Table 2). Therefore, different amounts of Cys were spiked to a sample and analyzed by the proposed method. The results of Cys determination in the human blood serum sample are given in Table 2. Satisfactory percentages of recovery were found for Cys in the experimental results.

4. Conclusion

In this research, a novel nanostructured composite material was explored based on HBX and the unique properties of MWCNT. The unique composite material may provide a good electrochemical sensing platform for redox biomolecules and is expected to have wide potential applications in direct electrochemistry, biosensors, and biocatalysts. CV and DPV investigations showed the effective electro-catalytic activity of the modified electrode in decreasing the anodic over-potential for the oxidation of Cys and the complete resolution of its anodic wave from Try. Compared with Cys responses at CPE, the electrochemical sensitivity of Cys at the proposed electrode was improved dramatically, revealing some advantages of HBX/MWCNT/CPE over CPE such as high conductivity and fast electron transfer. High sensitivity, selectivity as well as

reproducibility of the voltammetric responses, very low detection limit, and surface regeneration may be mentioned as the advantages of the proposed modified electrode.

Acknowledgments

The authors wish to thank Yazd University Research Council for its financial support of this research.

References

1 M. Mazloum Ardakani, A. Dehghani Firouzabadi, N. Rajabzadeh, M. A. Sheikh Mohseni , A. Benvidi and M. Abdollahi Alibeik*, J. Iran. Chem. Soc*, 2012**, 9,** 1.

2 M. Mazloum Ardakani, N. Rajabzadeh, A. Dehghani Firouzabadi, M. A. Sheikh Mohseni A. Benvidi, H. Naeimi, M. Akbari and A. Karshenas, *Anal Methods*, 2012, **4,** 2127.

3 M. Mazloum Ardakani, N. Rajabzadeh, A. Dehghani Firouzabadi and A. Benvidi. *Anal Methods*, 2014, in press.

4 M. Mazloum-Ardakani, H. Beitollahi, M. K. Amini, F. Mirkhalaf and M. Abdollahi-Alibeik, *Anal. Methods*, 2011, **3**, 673.

5 M. Mazloum-Ardakani, A. Talebi, H. Naeimi and M. A. SheikhMohseni, *Anal. Methods*, 2011, **3**, 2328.

6 M. Mazloum-Ardakani, Z. Taleat. H. Beitollahi and H. Naeimi, *Anal. Methods*, 2010, **2**, 149.

7 L. C. Jiang and W. D. Zhang. *Biosens. Bioelectron*, 2010, **25**, 1402.

8 C. B. Jacobs, M. J. Peairs and B. J. Venton, *Anal. Chim. Acta*, 2010, **662**, 105.

9 D. L. Nelson and M. M. Cox. *Lehninger Principles of Biochemistry*, 3th ed., Worth Publishers, USA, 2000.

10 S. Bridavari. *the Merck Index*, 11th ed., Merck and Co. Inc., New Jersey. 1989.

11 W. F. Ganong. *Review of Medical Physiology*, Prentice Hall, Englewood Cliffs, NJ. 1997.

12 A. Townshend, *Encyclopedia of Analytical Science*, 1995, Vol. 3, Academic Press, London, p.1735.

13 C. Lau, X. Qin, J. Liang and J. Lu. *Anal. Chim. Acta*, 2004, **514**, 45.

14 P. C. White, N. S. Lawrence, J. Davis and R.G. Compton. *Anal. Chim. Acta*, 2001**, 447**, 1.

15 S. Shahrokhian. *Anal. Chem,* 2001, **73**, 5972.

16 G. Chwatko and E. Bald. *Talanta,* 2000, **52**, 509.

17 H. Wang, W. S. Wang and H. S. Zhang. *Talanta,* 2001, **53**, 1015.

18 C. Zhao, J. Zhang and J. Song. *Anal. Biochem*, 2001, **297,** 170.

19 A. Jarosz-Wilkolazka, T. Ruzgas and L. Gorton. *Technol,* 2004, **35**, 238.

20 S. N. Young, F. R. Ervin, R. O. Phil and P. Finn. *Psychopharmacology,* 1989, **98**, 508.

21 K. Horwitt, C. C. Harvey, W. S. Rothwell, J. L. Cutler and D. Haffron. *J. Nutr*, 1956, **60,** 1.

22 V. Simonneaux and C. Ribelayga. *Pharmacol. Rev*, 2003, **55**, 325.

23 A. Babaei, M. Zendehdel, B. Khalilzadeh and A. Taheri. *Colloids Surf. B,* 2008, **66,** 226.

24 Z. D. Chen, J. X. Wei and W. C. Wang. *Chin. Chem. Lett*, 2010, **21,** 353.

25 M. Mazloum Ardakani, H. Beitollahi, Z. Taleat, H. Naeimi and N. Taghavinia. *J. Electroanal. Chem*, 2010, **644**, 1.

26 K. A. Frith and J. L. Limson. *Electrochim. Acta*, 2009, **54**, 3600.

27 M. Mazloum Ardakani, B. Ganjipour, H. Beitollahi, M. K. Amini, F. Mirkhalaf, H. Naeimi and M. Nejati-Barzoki. *Electrochim. Acta*, 2011, **56**, 9113.

28 B. F. Mirjalili, A. Bamoniri and M. A. Mirhoseini, *Chemistry of Heterocyclic Compounds*, 2012, **48**, 856.

29. M. Mazloum-Ardakani and A. Khoshroo. *Electrochim. Acta*, 2013, **103**:77.

30. H. Shiuh-Chuan Her and L. Chun-Yu . *Materials* 2013, ***6,*** 2274

31 M. Sharp, M. Petersson and K. J. Edstrom, *J. Electroanal. Chem*, 1979, **95***,* 123.

32 E. Laviron, *J. Electroanal. Chem*, 1979, **101***,* 19.

33 A. J. Bard, L. R. Faulkner, *Electrochemical Methods: Fundamentals and Applications*, 2nd ed., Wiley, New York, 2001**.**

34 A. A. Ensafi and S. Behyan. *Sens. Actuators B,* 2007, **122,** 282.

35 G. Shi, J. Lu, F. Xu, W. Sun, L. Jin, K. Yamamoto, S. Tao and J. Jin. *Anal. Chim. Acta,* 1999, **391**, 307.

36 A. Abbaspour and A. Ghaffarinejad. *Electrochim. Acta*, 2008, **53**:6643.

37 C. Deng, J. Chen, X. Chen, M. Wang, Z. Nie and S. Yao. *Electrochim. Acta*, 2009, **54,** 3298.

38 P. Limuthu and S. A. John. *Electrochem. Commun,* 2009, **11**, 367.

39 G. C. Miller and G. N. Miller. *Statistics for analytical chemistry*, 2nd ed, Ellis Harwood, Chichester. 1988.

Figure captions:

Fig.1. The scanning electron microscopy (SEM) images of CPE (A), CPE/MWCNT (B) and CPE/MWCNT/HDX (C).

Fig. 2. The infrared spectra of Graphite, Graphite/MWCNT and Graphite/MWCNT/HDX.

Fig. 3. The EDX spectra of Graphite, Graphite/MWCNT and Graphite/MWCNT/HDX.

Fig. 4. Cyclic voltammograms of HDX/MWCNT/CPE in a buffer solution (pH 8.5) for different scan rates; curves 1–6 correspond to: 10, 40, 80, 200, 400 and 600 mV s^{-1}. Insets: Variation of (A) I_p vs. the scan rate; (B) E_p vs. the logarithm of the scan rate in the range of 10–500 mV s^{-1} and (C) E_{pa} vs. pH.

Fig. 5. CVs of (a) unmodified CPE in a 0.1 M phosphate buffer solution (pH 8.5) at the scan rate of 100 mV s^{-1} ; (b) as (a) in the presence of 0.50 mM cysteine; (c) as (a) at the surface of HDX/CPE; (d) as (b) at the surface of HDX/CPE; (e) as (b) at the surface of HDX/MWCNT/CPE. Error bars are the mean of 3 measurements.

Fig. 6. CVs of HDX/MWCNT/CPE in a 0.1 M phosphate buffer solution (pH 8.5) for Cys concentrations of 0.04, 0.1, 0.2, 0.4 and 1.0 mM. Insets: (A) the Tafel plot derived from the

cyclic voltammogram at the scan rate of 100 mV s^{-1} (B) variation of the electrocatalytic currents vs. the square root of the scan rate. Error bars are the mean of 3 measurements.

Fig. 7. Chronoamperograms obtained at HDX/MWCNT/CPE in a 0.1 M phosphate buffer solution (pH 8.5) for Cys concentrations of 0.2, 0.4, 0.6, 0.8, 1.0 and 1.2 mM. Insets: (A) plots of I vs. $t^{-1/2}$ (B) plot of the slope of the straight lines (from inset B) against the Cys concentration.

Fig. 8. Differential pulse voltammograms plotted at HDX/MWCNT/CPE in a 0.1 M phosphate buffer solution (pH 8.5) containing different concentrations of Cys (from inner to outer): 0.01, 0.02, 0.04, 0.08, 0.2, 0.4 and 0.8 mM. Insets: plot of the peak current as a function of Cys concentration. Each point in the calibration plots is the mean of 3 measurements.

Fig. 9. Differential pulse voltammograms obtained at HDX/MWCNT/CPE in a 0.1 M phosphate buffer solution (pH 8.5) containing different concentrations of Cys and Try (from inner to outer): 0.01+0.01, 0.03+0.02, 0.06+0.04, 0.2+0.06, 0.35+0.08, 0.5+0.10 and 1.0+0.5 μM respectively. Inset: DPV plotted in a 0.1 M phosphate buffer solution (pH 8.5) containing 0.5 mM Cys + 0.1 mM Try at HDX/MWCNT/CPE (a) and at a bare CPE (c) respectively. DPV plotted in a 0.1 M phosphate buffer solution (pH 8.5) containing Cys=0.5 mM at HDX/MWCNT/CPE (b) and at a bare CPE (d) respectively.

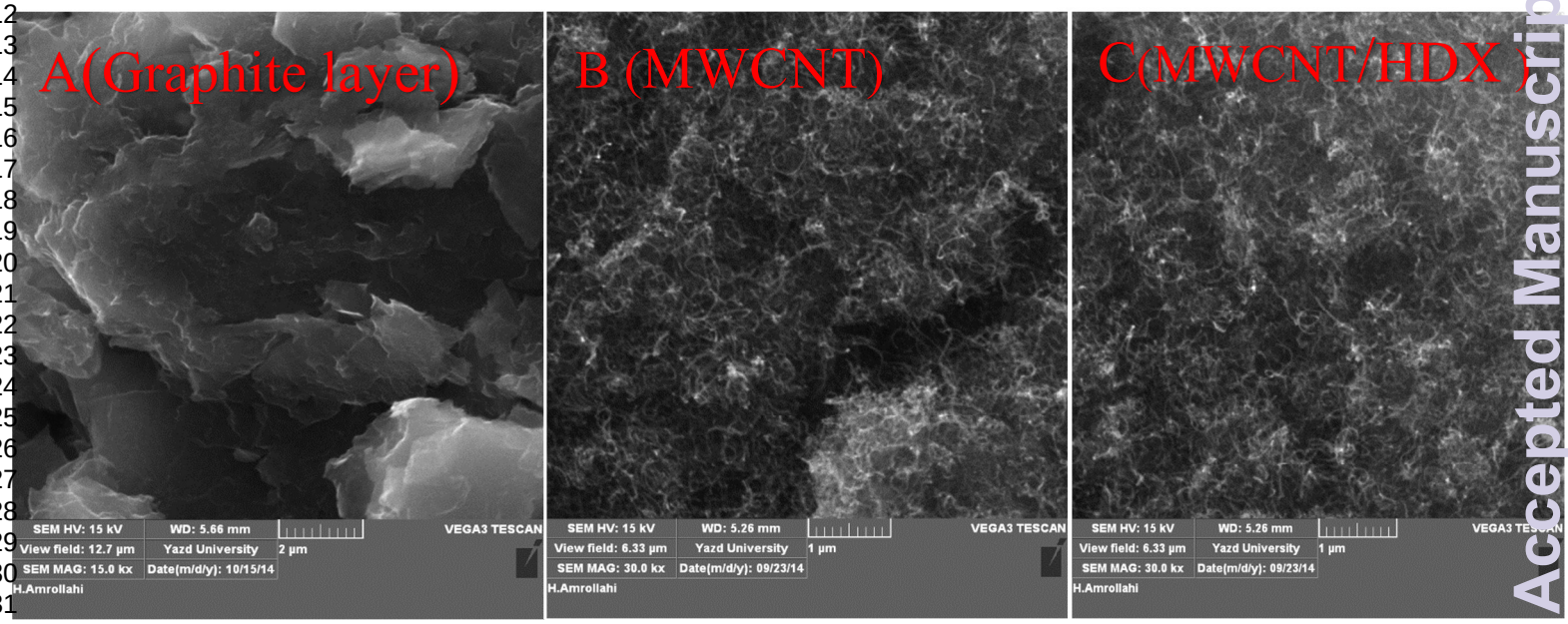

Fig. 1

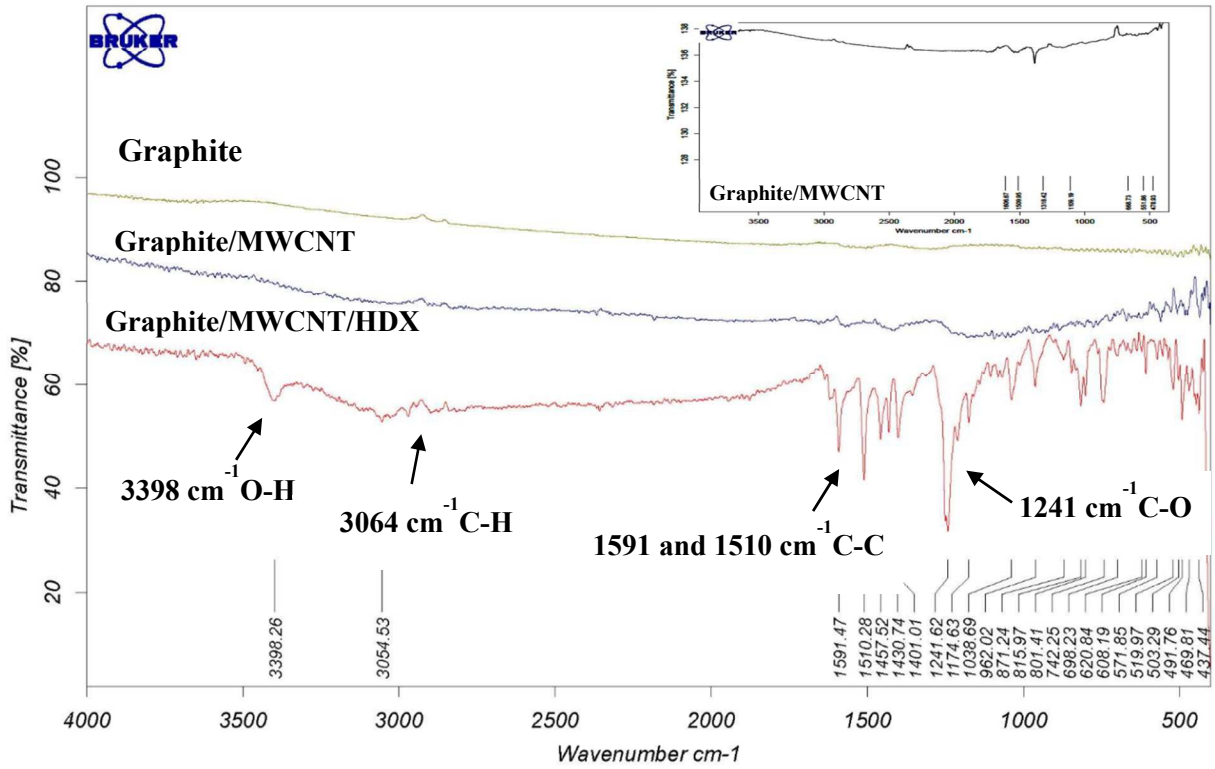

Fig. 2

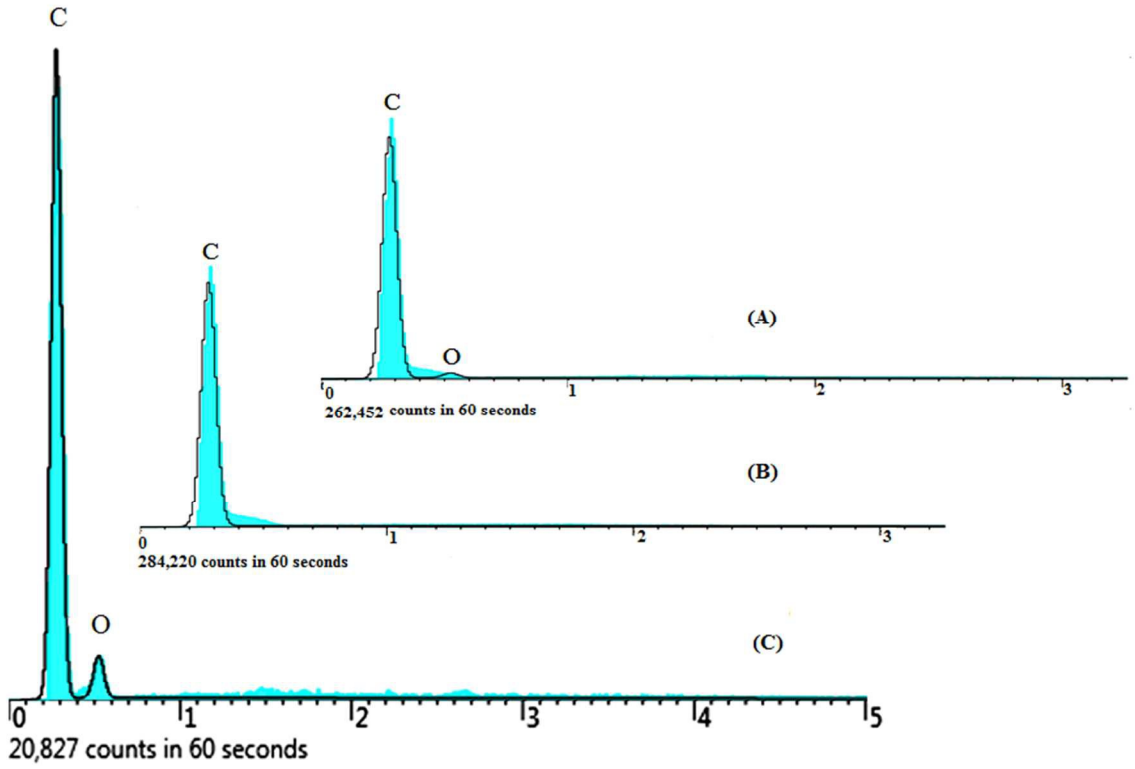

Fig. 3

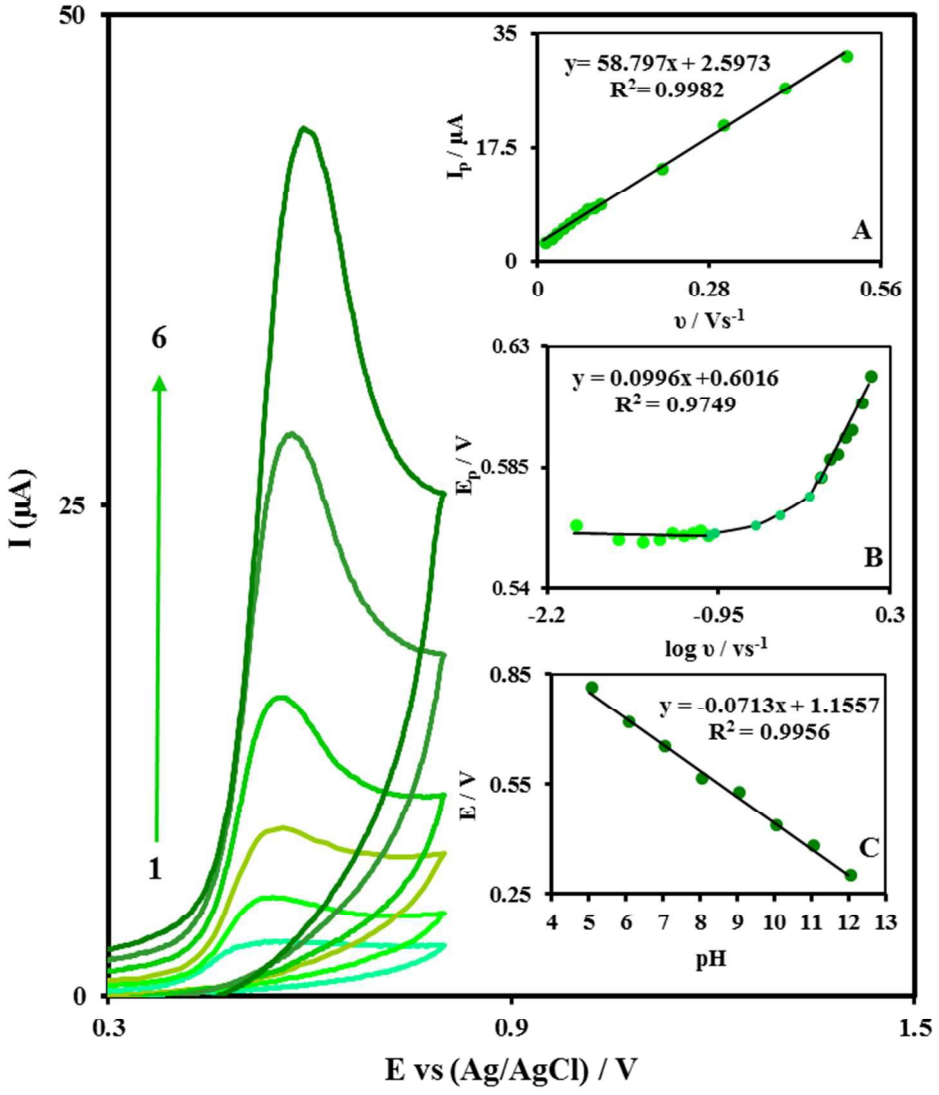

Fig. 4

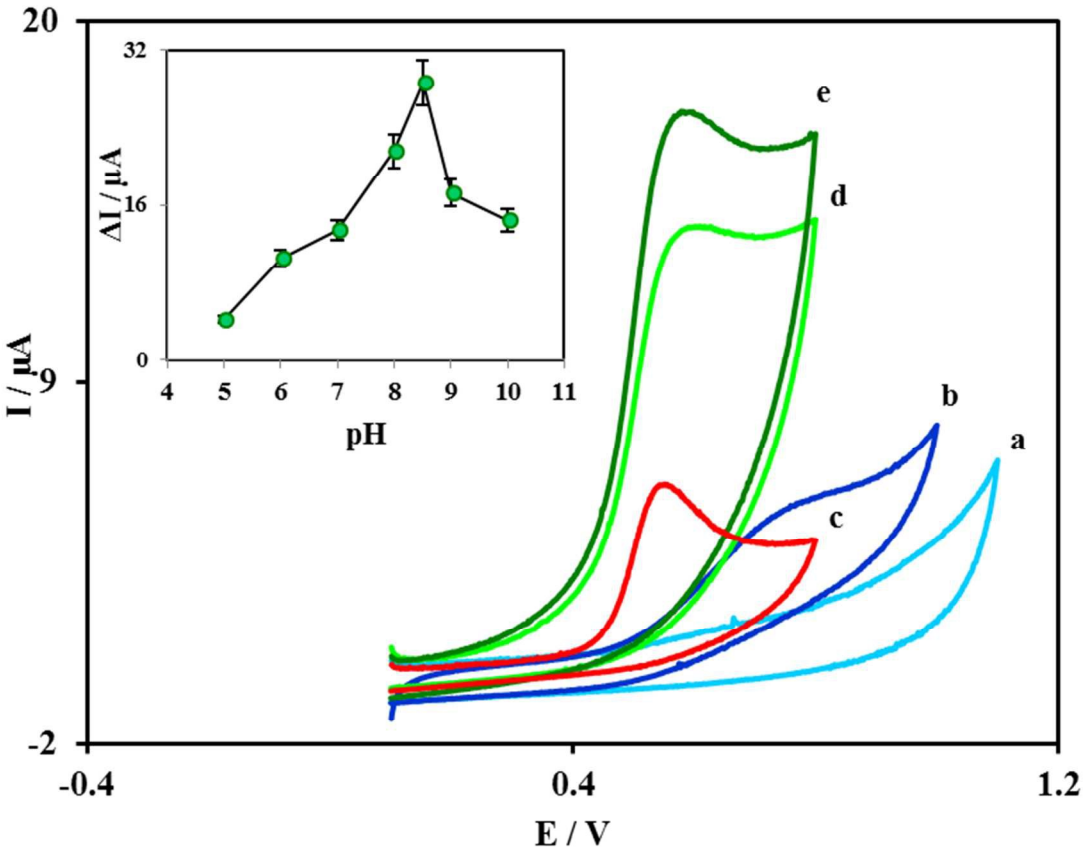

Fig. 5

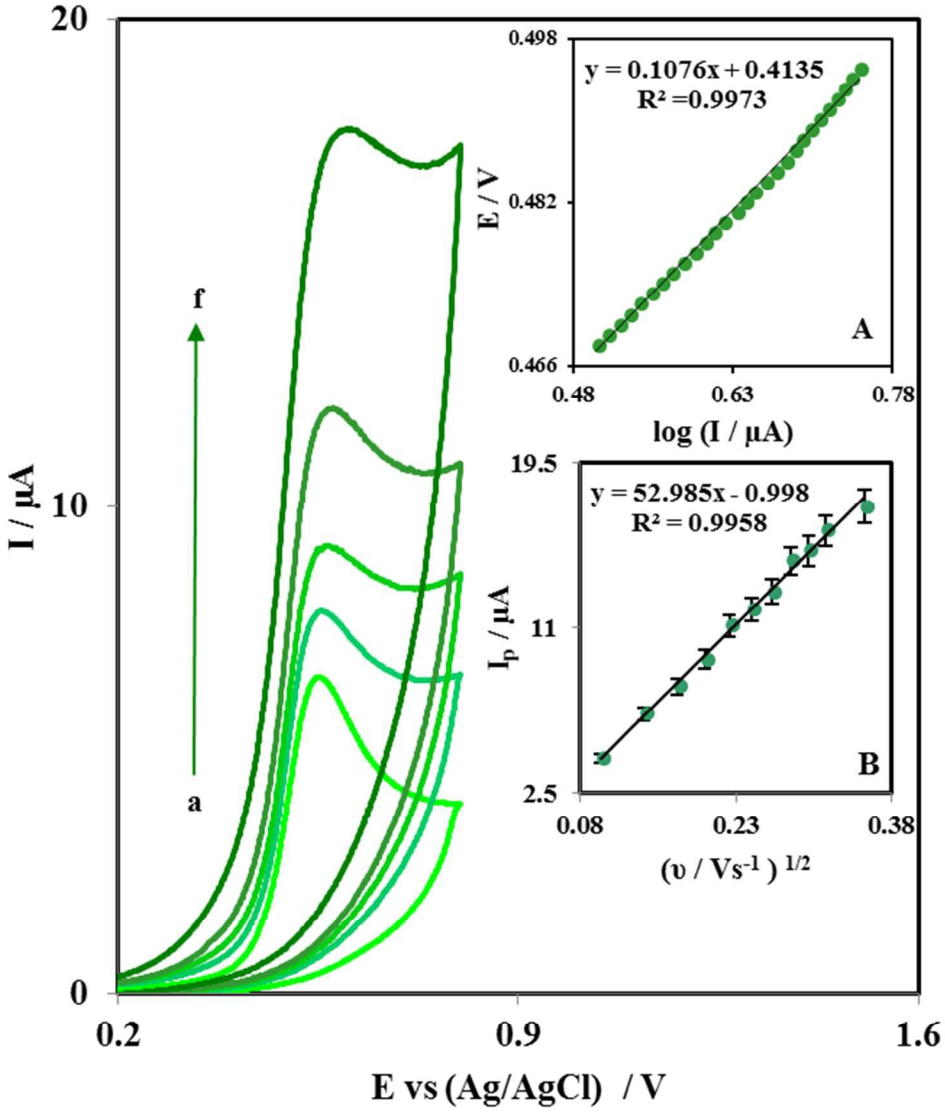

Fig. 6

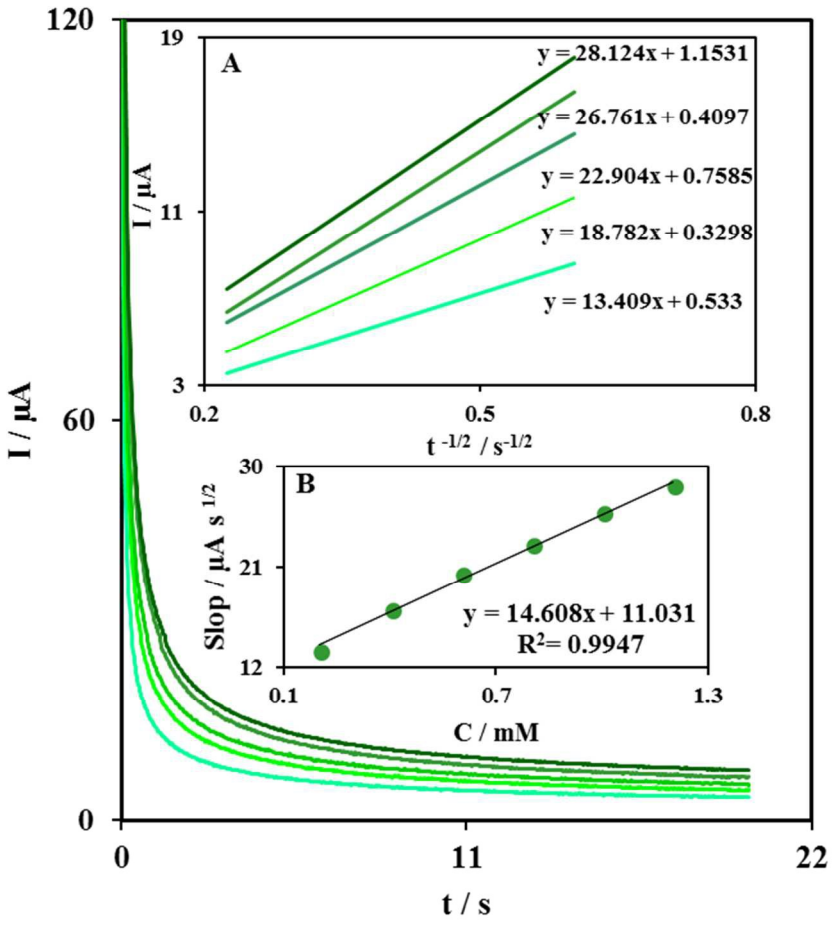

Fig. 7

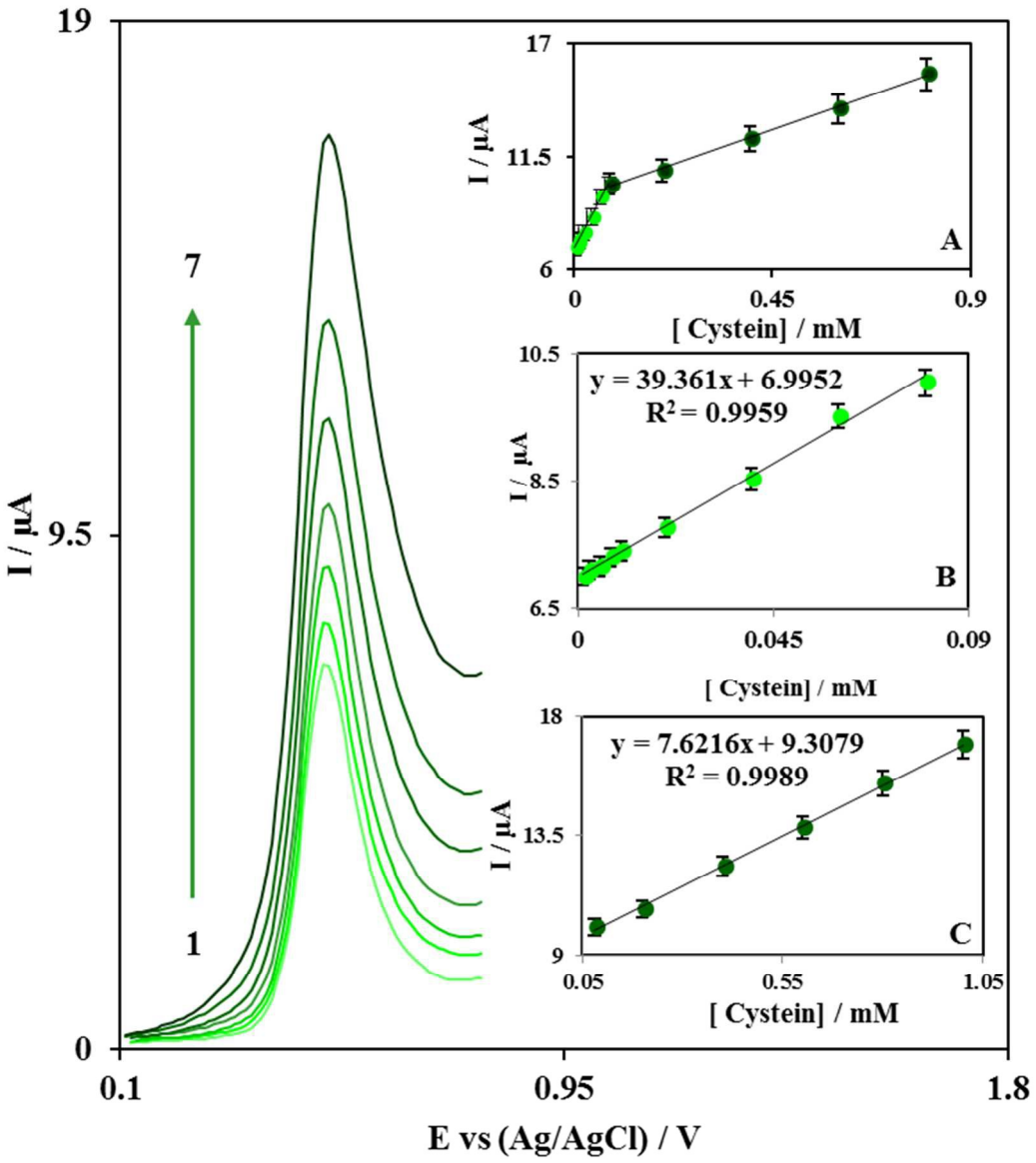

Fig. 8

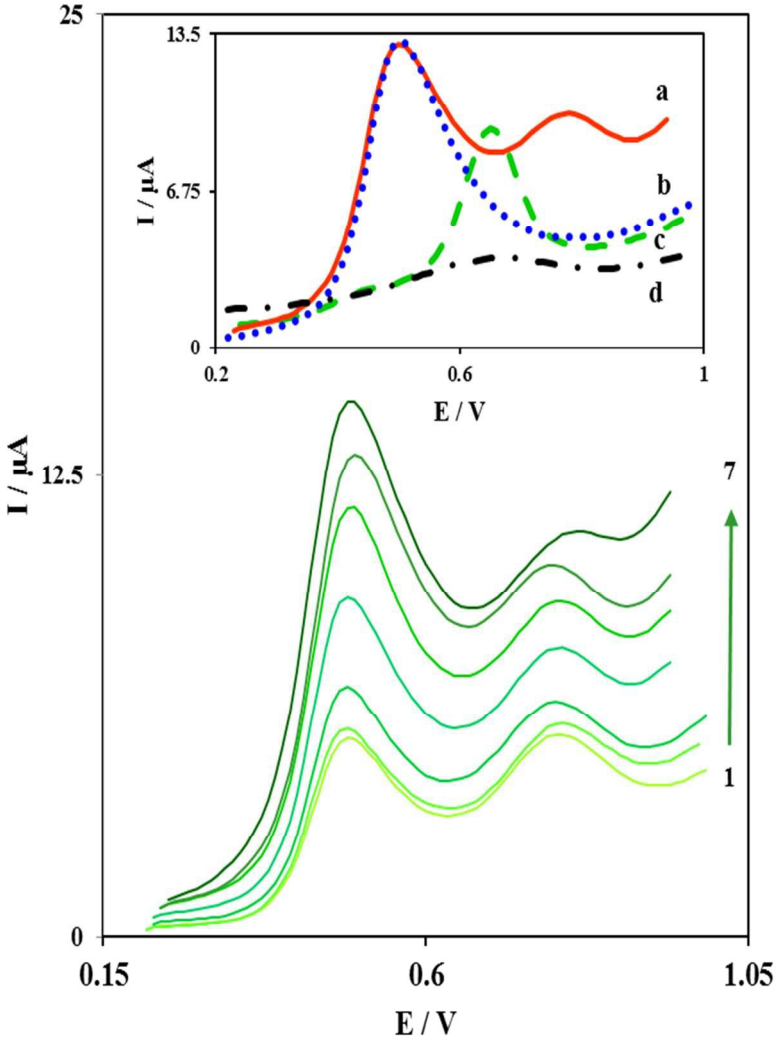

Fig. 9

Table 1. Comparison of some electrochemical procedures used in the determination of Cys

Electrode	Modifier	Detection limit (μM)	Linear range (μM)	pH	Oxidation potential (V)	Ref.
GCE	Nile blue A	1.3	10.0-250	10.0	0.390	34
GCE	Co – HCF	1.0	1.5-200.0	3.0	0.830	35
CPE	Cu-Co-HCF	4.0	6.0-100.0	2.0	0.740	36
GCE	[a]BCNT	0.26	7.8-200.0	7.4	0.47	37
GCE	[b]AMT	3.36	20.0-180.0	7.2	0.6	38
CPE	HBX/MWCNT	1.0	4.0-1000.0	8.5	0.50	This work

[a]Boron doped carbon nanotube

[b]5-amino-2-mercapto-1,3,4-thiadiazole

Table 2. The application of HBX/MWCNT/CPE for determination of Cys in human blood serum

Number	Initial concentration (mM)	Spiked (mM)	Founded (mM)	Recovery %
1	0.071	0.0	0.072	-
2	0.071	0.2	0.272	100.5
3	0.071	0.3	0.381	103.0
4	0.071	0.4	0.466	98.7
5	0.071	0.6	0.685	102.3

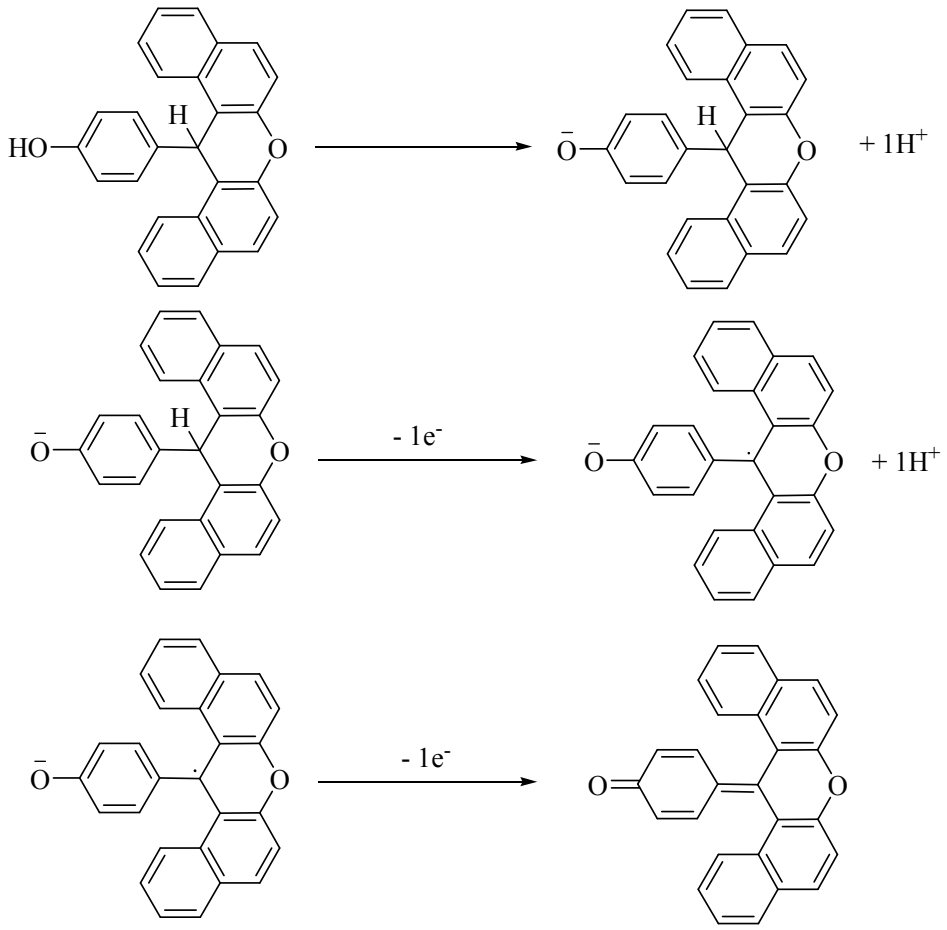

Scheme 1